Proceedings on Engineering Sciences

SOLVING CAUCHY PROBLEM FOR MODELLING THE DYNAMICS OF VEHICLE-FIXED BARRIER COLLISIONS BY THE FINITE ELEMENT METHOD AND THE EFFECT OF FORCES OF INERTIA ON PASSENGERS

Stanimir Karapetkov[1]
Hristo Uzunov
Silvia Dechkova
Vasil Uzunov

A B S T R A C T

Dynamic investigation of vehicle collisions with stationary obstacles in most cases concerns solutions to complex tasks related to identification of occupant position in the vehicle. The focus of the study is on how forces of inertia change their magnitude and direction during car motion. This requires specific analysis done by dividing vehicle trajectory into separate stages according to certain indicators, such as free motion, impact process, post-impact residual motion. Particular attention has been paid to the impact itself, in which the forces of inertia are the most intense, and their magnitude and direction change abruptly. Solution to Cauchy problem has been found, in which initial kinematic parameters of the crash process are considered, satisfying the kinematic values at rest position. Dynamic analysis of the impact phase of a vehicle-fixed barrier collision has been performed by the finite element method using the software product Abaqus/Explicit.

1. DYNAMIC MODEL OF A VEHICLE-FIXED BARRIER FRONT CRASH (ALL CAPS

The present dynamic investigation in this study is related to the car motion when a driver loses control, followed by a collision process with a roadside tree and the subsequent post-impact vehicle motion. The purpose of this investigation is to design a mechanical and mathematical model so as to analyse the vehicle dynamic motion and the impact process itself (Lyubenov et al., 2019, 2022; Saliev & Damyanov, 2022). Futhermore, it aims at determining directions and magnitudes of the forces of inertia exerted on the bodies in the car at each stage, predicting in a dynamic aspect the displacement of the vehicle occupants in the car body (Uzunov, Dechkova, Dimitrov, Uzunov, 2021; Matzinski et al., 2021).

Corresponding author: Stanimir Karapetkov
Email: skarapetkov@yahoo.com

Forces of inertia act in different stages and they are of various types and magnitudes so the car motion is divided into several stages. The first stage is prior to impact, the second is the impact itself and the third is the post-impact motion. The tasks studied are related to both modelling vehicle dynamics in each stage, as well as the displacement of the bodies in the movable coordinate system. Furthermore, the effect of the forces of inertia on the passengers in the car is investigated and their directions are determined in order to identify their displacement. Inertial forces cause relative displacement of the bodies inside the car body, and the size of displacement depends on the fact whether the passanger vehicle occupants use seat belts or not.

According to D'Alembert's principle, the first main force acting on bodies and considered in the vehicle's movable coordinate system is the fictitious translation force. It is determined by the expressionand

$$\vec{F}_e = -m.\vec{a}_e = -m.[\vec{a}_c + \vec{\varepsilon} \times \vec{\rho} + \vec{\omega} \times \vec{\omega} \times \vec{\rho}]. \qquad (1)$$

where m is the mass of the passenger; $\vec{a}_e$ - fictitious translation acceleration; $\vec{a}_c$ - acceleration of vehicle's center of mass; $\vec{a}_{cc}$ - Coriolis acceleration of the body center of mass; $\vec{\omega}$ - angular velocity of the vehicle; $\vec{\varepsilon}$ - vehicle angular acceleration; $\vec{\rho}$ - radius vector of the body center of mass relative to the vehicle's center of mass.

Another major inertial force acting on the bodies in the car when there is body displacement and the car rotates around its vertical axis is the Coriolis inertial force. It is of the type

$$\vec{F}_c = -m.\vec{a}_{cc} = -2.m.[\vec{\omega} \times \vec{V}_r], \qquad (2)$$

where $\vec{V}_r$ - relative velocity of the body center of mass in relation to the vehicle movable coordinate system.

During vehicle deceleration motion at the stage of loss of transverse stability main force is exerted on the bodies, namely the fictitious translation force caused by the retarded motion. It has the form of

$$\vec{F}_{ec} = -m.\vec{j}_e, \qquad (3)$$

$\vec{j}_e$ – fictitious translation acceleration in retarded mode.

Centrifugal force caused by inertia is generated when the vehicle rotates. The magnitude of the inertia force depends on the three-component rotation and the direction of the vector $\vec{\omega}$. To facilitate the analysis, it is assumed that the car rotation has a major component around the vertical axis passing through the center of mass. The magnitude of the centrifugal inertial force is as follows:

$$\vec{F}_{e\omega} = m.\omega^2.\vec{\rho}, \qquad (4)$$

where $\vec{\rho}$ is the distance from the body center of mass to the vehicle center of mass. This distance is variable and depends on the distance of the body center of mass to the vehicle center of mass in the movable coordinate system.

To achieve the aim of the dynamic investigation and to determine the body motion, it is necessary to look into the car macromotion in the separate stages in advance: prior the impact, the impact itself and after the impact (Jiang et al., 2003; Karapetkov & Dimitrov, 2022; Karapetkov 2010; Karapetkov & Uzunov 2016; Karapetkov et al., 2019). Solution to the Cauchy problem is found in which the initial conditions of each stage are the final ones of the previous one, satisfying the kinematic parameters of the known position at rest (Karapetkov et al., 2019). At impact stage, the task is solved by using the finite element method, and the conditions satisfy the direction of deformation of the car body and the direction of the impact force.

For certain kinematic quantities in the stages of motion, the magnitudes and directions of each component of the inertial forces could be sufficiently predicted, including their total magnitude as a vector. The study predicts the possible components of the inertial forces that have caused a change in the occupant direction of motion in the way that they have acquired motion in a given direction and have reached a certain final position at rest. During displacement, known and found parameters are compared, such as the final position of the passenger's body, provided oral evidence and characteristic injuries to the body. The presence of discrepancies also determines the insolvency of legal defenses in effort to transfer responsibility to the passenger killed in the road accident.

An example of a road accident with a Mercedes is given where the driver loses control, crosses the lane, leaves the road and hits a roadside tree. In the event of the traffic accident, one of the passengers is in a state of final rest position outside the car.

Characteristics and main signs of road accidents of such types are tyre traces prior the impact in cases of loss of control, typical deformations and dents of the car's contact with the roadside tree, the established final rest positions of the vehicle, the scattered objects at the impact phase and the body of the deceased car occupant. At the first stage of motion, the car was moving with relatively transverse friction between the tyres and the road surface, and the motion trajectory was a circular arcuate path. The car crossed the entire lane obliquely and what followed was the impact with the roadside tree (Fig. 1 and Fig. 2) (Daily et al., 2006; Schmidt et al., 1998; Sharma et al., 2007; Wach, 2003).
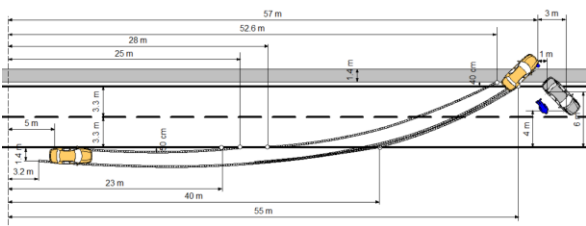
Figure 1. Scheme of the road accident

Figure 2. Post-impact position of vehicle and passengers involved in the car accident

Contact with the tree results in characteristic deformations in the area of the engine compartment, the shape of which resembles that of the tree trunk (Uzunov et al., 2022).

In addition to the analysed deformation area in the front of the vehicle and the front door, a characteristic swell has been found on the surface, which was inside out related to the car's coordinate system, invariably fixed to its center of mass (Fig. 3). The direction of deformation of this element of the body does not correspond to the direction of deformation from the contact with the tree. This means that the nature and intensity of the deformation is a sign of force action caused by the vehicle motion in the phase of the accident. The analysis requires answers to significant questions which concern the forces that have caused the damage, the reasons and the derormer of that particular element of the car body.

The answer to this question can be obtained by studying the macromotion of the car in three separate phases - the phase of loss of transverse stability prior the impact, the impact phase and the phase of post-impact vehicle motion (Uzunov, Matzinski. Dechkova, Dimov, 2021). Technical data for the Mercedes-Benz E-Class (W124): length $4740\ mm$; width $1740\ mm$; height $1430\ mm$;

wheelbase $2800\ mm$; front trace $1501\ mm$; rear trace $1491\ mm$; gross vehicle weight $1520\ kg$; Moment of inertia about the vertical axis $J_z = 2460\ kg.m^2$.

Figure 3. Deformations on the car

The coordinates of the vehicle center of mass at the time of impact and the angle of rotation about the vertical axis of the vehicle, relative to the selected fixed coordinate system, are:

$$x_c = 55,1\ m;\ x_c = 4,9\ m;\ \varphi_z = 45^o. \qquad (5)$$

The velocity of the center of mass at the moment of impact relative to the mobile coordinate system, invariably fixed to the vehicle is:

$$V_{x\prime} = 51,5\ km/h;\ V_{y\prime} = 39,7\ km/h. \qquad (6)$$

2. RESULTS OF THE DYNAMIC STUDY

The impact itself is considered by the finite element method through the software product Abaqus/Explicit (Fig.4 and Fig.5). (Kolev & Kadirova, 2018; 2019). The Cauchy problem is solved, in which a solution is found regarding the depth of deformation in the right-lateral front part, as well as data on the initial conditions of the kinematic quantities satisfying the final vehicle position at rest in post-impact macromotion.

The change in the center of mass velocity at the impact stage is shown in the graphical dependences (Fig. 6 - 7).

The dynamic study of the impact phase and the resulting final conditions determine the initial conditions of the car's macromovement after the impact. The distance from the center of mass after impact and the angle of rotation relative to the vertical axis are taken into account.
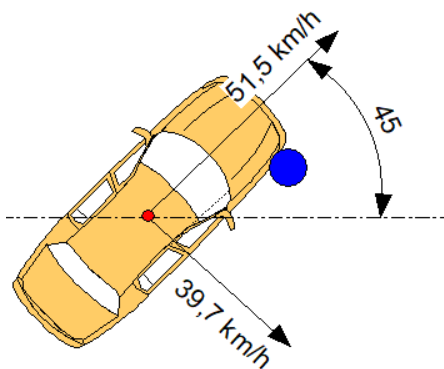
a) Initial location of collision point
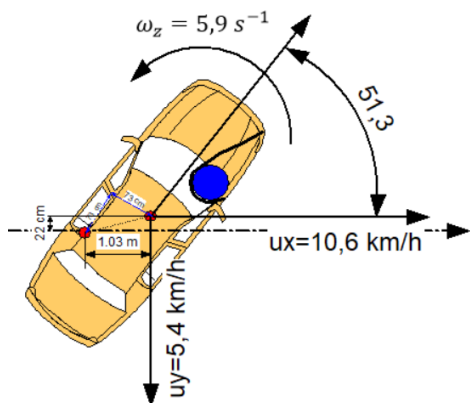
b) Post-impact location
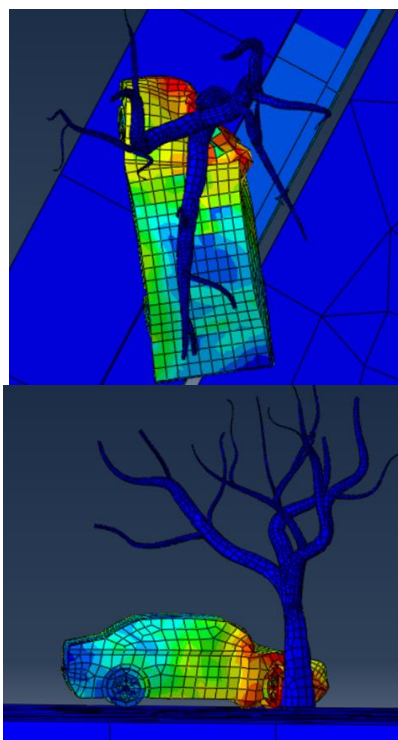
Figure 4. Post-impact vehicle location

Figure 5. Impact deformation between car and tree through software product Abaqus/Explicit
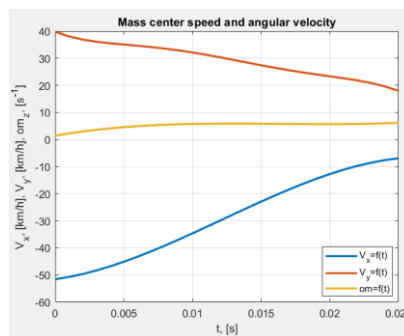

Figure 6. Change of the projections of the velocity of the center of mass and the angular velocity about the vertical axis at impact stage
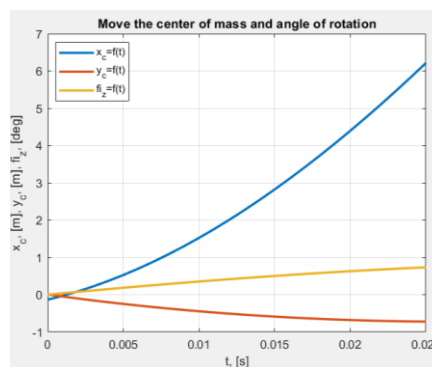

Figure 7. Change of the coordinates of the center of mass and angle of rotation about the vertical axis at impact phase

The distance traveled in the impact phase, the angle of rotation and the change in velocities of the center of mass is:

$$u_{xc} = 4,85 \ m/s \,; \ u_{yc} = -2,6 \ m/s \,;$$
$$\omega_z = 5,9 \ s^{-1}; \tag{7}$$
$$x_c = 3,33 \ m; \ y_c = 4,42 \ m; \ \varphi_z = 51,3^o.$$

Macro simulation of vehicle motion in case of loss of lateral stability is observed in an arbitrarily accepted absolute coordinate system $OXYZ$ (Niehoff & Gabler, 2006; Owsiański, 2007; Stronge, 2000; Dechkova, 2018). To study the car motion, it has been assumed that its own coordinate system $Cx'y'z'$ is movable and permenantly connected to the vehicle center of mass C (Fig. 8). In addition, a permanently connected $Cxyz$ coordinate system is attached to it, parallel to the absolute and translationally movable one.

Coordinates of the vehicle center of mass $C \ x_c, y_c, z_c$ in the fixed coordinate system are selected for generalized coordinates of the car motion. Rotational motion of the car is expressed by the Euler transformations and corresponding angles, namely ψ, θ and φ. The precession angle of ψ, taking into account the rotation around the axis Cz; respectively, the angular velocity of $\dot{\psi}$ is obtained; the angle θ of nutation, taking into

account the rotation with respect to the axis $C\rho$, the intersection of the planes Oxy and $Cx'y$.

Therefore, the force of gravity $\vec{G}$ will lie on the axis Oz. The spatial arrangement model of the car is a plane located on four elastic supports, which are marked by $K_i(i = 1 \div 4)$ (Fig. 9).
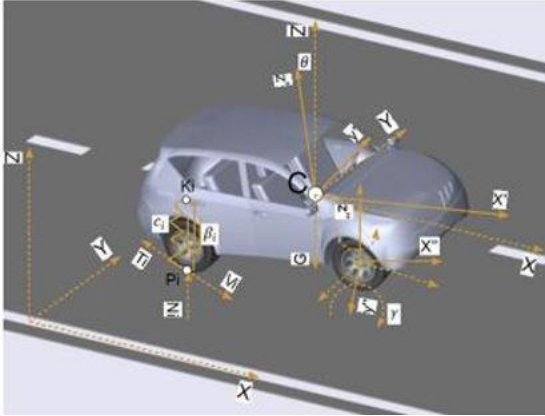

Figure 8. Spatial dynamic model of an automobile with elastic suspension

$\vec{F}_i(i = 1 \div 4)$ is elastic force generated by the elasticity of tires and springs; $\vec{N}_i(i = 1 \div 4)$ is normal reaction at the contact point of automobile tires, corresponding to elastic force; $\vec{V}_i(i = 1 \div 4)$ is velocity of the contact point P_i in the plane of the road Oxy; $\vec{T}_i(i = 1 \div 4)$ is friction force at the contact points that lies in the plane of the road Oxy; $\vec{R}_i(i = 1 \div 4)$ is resistance force generated by damping elements in suspension; $c_i, \frac{N}{m}(i = 1 \div 4)$ elasticity of suspension, taking into account both

coefficient of elasticity of tires and suspension; $b_i, \frac{N \cdot s}{m}(i = 1 \div 4)$ coefficient of linear resistance.

The car motion according to the studies of kinetic energy and generalized forces is defined by six differential equations with six generalized coordinates. These equations are valid if the friction force is in accordance with Coulomb's law and the wheels slide on the ground without rolling. According to (12), the wheels keep a continuous contact with the road .

Generalized forces and moments in the right-hand sides of the differential equations (9) are determined by assuming that the absolute coordinate system has a vertical axis of Oz
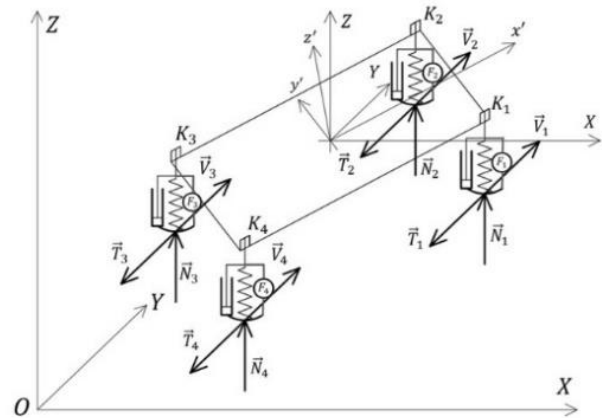

Figure 9. Model of the forces acting on a car in its spatial motion, taking into account the elasticity of tires (suspension)

$$m \cdot \ddot{x} = \left[\sum_{i=1}^{4} F_{xi}\right]; \quad m \cdot \ddot{y} = \left[\sum_{i=1}^{4} F_{yi}\right]; \quad m \cdot \ddot{z} = \left[-G + \sum_{i=1}^{4} N_i - \sum_{i=1}^{4} R_i\right]; \tag{8}$$

$$a_{11} \cdot \ddot{\varphi} + a_{12} \cdot \ddot{\psi} + a_{13} \cdot \ddot{\theta} =$$

$$\left\{ \begin{array}{c} \sum_{i=1}^{4} N_i \cdot \delta_{\varphi i} + \sum_{i=1}^{4}\left(F_{xi} \cdot f_{\varphi_x} + F_{yi} \cdot f_{\varphi_y}\right) - \sum_{i=1}^{4} R_i \cdot \delta_{\varphi i} \\ -b_{11} \cdot \dot{\varphi}^2 - b_{12} \cdot \dot{\psi}^2 - b_{13} \cdot \dot{\theta}^2 - c_{11} \cdot \dot{\varphi} \cdot \dot{\psi} - c_{12} \cdot \dot{\varphi} \cdot \dot{\theta} - c_{13} \cdot \dot{\psi} \cdot \dot{\theta} \end{array} \right\};$$

$$a_{21} \cdot \ddot{\varphi} + a_{22} \cdot \ddot{\psi} + a_{23} \cdot \ddot{\theta} =$$

$$= \left\{ \begin{array}{c} \sum_{i=1}^{4}\left(F_{xi} \cdot f_{\psi_x} + F_{yi} \cdot f_{\psi_y}\right) - b_{21} \cdot \dot{\varphi}^2 - b_{22} \cdot \dot{\psi}^2 - b_{23} \cdot \dot{\theta}^2 - \\ -c_{21} \cdot \dot{\varphi} \cdot \dot{\psi} - c_{22} \cdot \dot{\varphi} \cdot \dot{\theta} - c_{23} \cdot \dot{\psi} \cdot \dot{\theta} \end{array} \right\}; \tag{9}$$

$$a_{31} \cdot \ddot{\varphi} + a_{32} \cdot \ddot{\psi} + a_{33} \cdot \ddot{\theta} =$$

$$= \left\{ \begin{array}{c} \sum_{i=1}^{4} N_i \cdot \delta_{\theta i} + \sum_{i=i}^{4}\left(F_{xi} \cdot f_{\theta_x} + F_{yi} \cdot f_{\theta_y}\right) - \sum_{i=1}^{4} R_i \cdot \delta_{\theta i} - \\ -b_{31} \cdot \dot{\varphi}^2 - b_{32} \cdot \dot{\psi}^2 - b_{33} \cdot \dot{\theta}^2 - c_{31} \cdot \dot{\varphi} \cdot \dot{\psi} - c_{32} \cdot \dot{\varphi} \cdot \dot{\theta} - c_{33} \cdot \dot{\psi} \cdot \dot{\theta} \end{array} \right\};$$

$$a_{11} = J_{z'z'}; \quad a_{12} = -J_{z'z'} \cdot cos\theta - J_{z'x'} \cdot sin\varphi \cdot sin\theta - J_{y'z'} \cdot cos\varphi \cdot sin\theta;$$

$$a_{13} = -J_{z'x'} \cdot cos\varphi + J_{y'z'} \cdot sin\varphi;$$

$$b_{11} = 0; \quad b_{12} = \begin{pmatrix} -\dfrac{1}{2} \cdot sin2\varphi \cdot sin^2\theta \cdot \left(J_{x'x'} + J_{y'y'} \right) + \\ + J_{x'y'} \cdot cos2\varphi \cdot sin^2\theta + \\ + \dfrac{1}{2} \cdot sin2\theta \cdot \left(J_{z'x'} \cdot cos\varphi - J_{y'z'} \cdot sin\varphi \right) \end{pmatrix};$$

$$b_{13} = \left(\frac{1}{2} \cdot \left(J_{x'x'} - J_{y'y'} \right) \cdot sin2\varphi - J_{x'y'} \cdot cos2\varphi \right);$$

$$c_{11} = 0; \quad c_{12} = 0; \quad c_{13} = \begin{pmatrix} cos2\varphi \cdot sin\theta \cdot \left(J_{x'x'} + J_{y'y'} \right) - \\ - J_{z'z'} \cdot sin\theta - \\ -2 \cdot \begin{pmatrix} J_{x'y'} \cdot sin2\varphi \cdot sin\theta + \\ + J_{z'x'} \cdot sin\varphi \cdot cos\theta + \\ + J_{y'z'} \cdot cos\varphi \cdot cos\theta \end{pmatrix} \end{pmatrix}$$

$$a_{21} = \left(J_{z'z'} \cdot cos\theta - J_{z'x'} \cdot sin\varphi \cdot sin\theta - J_{y'z'} \cdot cos\varphi \cdot sin\theta \right);$$

$$a_{22} = \begin{pmatrix} J_{x'x'} \cdot sin^2\varphi \cdot sin^2\theta + J_{y'y'} \cdot cos^2\varphi \cdot sin^2\theta + \\ + J_{z'z'} \cdot cos^2\theta - J_{x'y'} \cdot sin2\varphi \cdot sin^2\theta \\ - J_{x'z'} \cdot sin\varphi \cdot sin2\theta - J_{y'z'} \cdot cos\varphi \cdot sin2\theta \end{pmatrix};$$

$$a_{23} = \begin{pmatrix} 0{,}5 \cdot J_{x'x'} \cdot sin2\varphi \cdot sin\theta - \dfrac{1}{2} \cdot J_{y'y'} \cdot sin2\varphi \cdot sin\theta - \\ - J_{x'y'} \cdot cos2\varphi \cdot sin\theta - J_{z'x'} \cdot cos\varphi \cdot cos\theta + \\ + J_{y'z'} \cdot sin\varphi \cdot cos\theta \end{pmatrix};$$

$$b_{21} = \left(-J_{z'x'} \cdot cos\varphi + J_{y'z'} \cdot sin\varphi \right) \cdot sin\theta;$$

$$b_{22} = 0; \quad b_{23} = \begin{pmatrix} \begin{pmatrix} 0{,}5 \cdot J_{x'x'} \cdot sin2\varphi - \dfrac{1}{2} \cdot J_{y'y'} \cdot sin2\varphi - \\ - J_{x'y'} \cdot cos2\varphi \end{pmatrix} \cdot cos\theta + \\ + \left(J_{z'x'} \cdot cos\varphi - J_{y'z'} \cdot sin\varphi \right) \cdot sin\theta \end{pmatrix};$$

$$c_{21} = \begin{pmatrix} \left(J_{x'x'} \cdot sin2\varphi - J_{y'y'} \cdot sin2\varphi - 2 \cdot J_{x'y'} \cdot cos2\varphi \right) \cdot sin^2\theta - \\ - \left(J_{z'x'} \cdot cos\varphi - J_{y'z'} \cdot sin\varphi \right) \cdot sin2\theta \end{pmatrix};$$

$$c_{22} = \begin{pmatrix} \left(J_{x'x'} \cdot cos2\varphi - J_{y'y'} \cdot cos2\varphi + 2 \cdot J_{x'y'} \cdot sin2\varphi \right) \cdot sin\theta - \\ - J_{z'z'} \cdot sin\theta \end{pmatrix};$$

$$c_{23} = \begin{pmatrix} \left(J_{x'x'} \cdot sin^2\varphi + J_{y'y'} \cdot cos^2\varphi - J_{x'y'} \cdot sin2\varphi - J_{z'z'} \right) \cdot sin2\theta - \\ -2 \cdot \left(J_{z'x'} \cdot sin\varphi + J_{y'z'} \cdot cos\varphi \right) \cdot cos2\theta \end{pmatrix};$$

$$a_{31} = J_{z'x'} \cdot cos\varphi + J_{y'z'} \cdot sin\varphi;$$

$$a_{32} = \begin{bmatrix} 0{,}5 \cdot \left(J_{x'x'} - J_{y'y'} \right) \cdot sin2\varphi \cdot sin\theta - J_{x'y'} \cdot cos2\varphi \cdot sin\theta - \\ - J_{z'x'} \cdot cos\varphi \cdot cos\theta + J_{y'z'} \cdot sin\varphi \cdot cos\theta \end{bmatrix};$$

$$a_{33} = J_{x'x'} \cdot cos^2\varphi + J_{y'y'} \cdot sin^2\varphi + \frac{1}{2} \cdot J_{x'y'} \cdot sin2\varphi; \quad b_{31} = J_{z'x'} \cdot sin\varphi + J_{y'z'} \cdot cos\varphi;$$

$$b_{32} = \begin{bmatrix} -\left[0.5 \cdot \begin{pmatrix} J_{x'x'} \cdot sin^2\varphi + J_{y'y'} \cdot cos^2\varphi + \\ + J_{z'z'} - J_{x'y'} \cdot sin2\varphi \end{pmatrix}\right] \cdot sin2\theta + \\ + (J_{z'x'} \cdot sin\varphi + J_{y'z'} \cdot cos\varphi) \cdot cos2\theta \end{bmatrix}; \quad b_{33} = 0;$$

$$c_{31} = \begin{bmatrix} [(J_{x'x'} + J_{y'y'}) \cdot cos2\varphi + 2 \cdot J_{x'y'} \cdot sin2\varphi + J_{z'z'}] \cdot sin\theta + \\ + 2 \cdot (J_{z'x'} \cdot sin\varphi + J_{y'z'} \cdot cos\varphi) \cdot cos\theta \end{bmatrix};$$

$$c_{32} = [(-J_{x'x'} + J_{y'y'}) \cdot sin2\varphi + 2 \cdot J_{x'y'} \cdot cos2\varphi]; \quad c_{33} = 0$$

We substitute the equations before $\delta_{\varphi i}$ and $\delta_{\theta i}$ using the notation

$$\delta_{\varphi i} = [(cos\varphi \cdot sin\theta) \cdot x'_{ki} + (-sin\varphi \cdot sin\theta) \cdot y'_{ki}];$$
$$\delta_{\theta i} = [(sin\varphi \cdot cos\theta) \cdot x'_{ki} + + (cos\varphi \cdot cos\theta) \cdot y'_{ki} + (-sin\theta) \cdot z'_{ki}].$$
(10)

To facilitate notation, substitution has been done, which looks like as follows:

$$f_{\psi xi} = \begin{bmatrix} \begin{pmatrix} -sin\psi \cdot cos\varphi - \\ -cos\psi \cdot sin\varphi \cdot cos\theta \end{pmatrix} \cdot \delta x'_{ki} + \\ + \begin{pmatrix} sin\psi \cdot sin\varphi - \\ -cos\psi \cdot cos\varphi \cdot cos\theta \end{pmatrix} \cdot \delta y'_{ki} + \\ + (-cos\psi \cdot sin\theta) \cdot \delta z'_{ki} \end{bmatrix}; \quad f_{\theta xi} = \begin{bmatrix} (sin\theta \cdot sin\psi \cdot sin\varphi) \cdot \delta x'_{ki} + \\ + (sin\theta \cdot sin\psi \cdot cos\varphi) \cdot \delta y'_{ki} + \\ + (-cos\theta \cdot sin\psi) \cdot \delta z'_{ki} \end{bmatrix}$$

$$f_{\varphi yi} = \begin{bmatrix} \begin{pmatrix} -sin\psi \cdot sin\varphi + \\ +cos\psi \cdot sin\varphi \cdot cos\theta \end{pmatrix} \cdot \delta x'_{ki} + \\ + \begin{pmatrix} -sin\psi \cdot cos\varphi - \\ -cos\psi \cdot sin\varphi \cdot cos\theta \end{pmatrix} \cdot \delta y'_{ki} \end{bmatrix}; \quad f_{\psi yi} = \begin{bmatrix} \begin{pmatrix} cos\psi \cdot cos\varphi - \\ -sin\psi \cdot sin\varphi \cdot cos\theta \end{pmatrix} \cdot \delta x'_{ki} + \\ + \begin{pmatrix} -cos\psi \cdot sin\varphi - \\ -sin\psi \cdot cos\varphi \cdot cos\theta \end{pmatrix} \cdot \delta y'_{ki} + \\ + (sin\psi \cdot sin\theta) \cdot \delta z'_{ki} \end{bmatrix}$$
(11)

$$f_{\theta yi} = \begin{bmatrix} (-cos\psi \cdot sin\varphi \cdot sin\theta) \cdot \delta x'_{ki} + \\ + (-cos\psi \cdot cos\varphi \cdot sin\theta) \cdot \delta y'_{ki} + \\ + (-cos\psi \cdot sin\theta) \cdot \delta z'_{ki} \end{bmatrix}$$

The relative motion of the wheels, the differential(s) and the engine are characterized by a system of four differential equations derived by the Lagrangian method, which has the form of

$$[I_\gamma] \cdot [\ddot{\gamma}] = [M_{\gamma i}]; \quad M_{\gamma i} = \{F_{i\tau} \cdot r_i + sign(\dot{\gamma}_i) \cdot [M_{di} - f_i \cdot N_i - M_{si}]\}$$
(12)

$\vec{F}_{i\tau}$ is tangential component of the tire-road friction force, the positive direction of which is taken backwards, in the more frequent cases of braking or loss of stiffness.

Where μ is friction coefficient depending on slipping speed on the contact spot; $\vec{r}_i$ – radius of the wheel; f_i – coefficient of rolling friction; $\vec{N}_i$ – normal reaction of the road on wheels; $[I_\gamma]$ - a square matrix of coefficients in front the actual angular acceleration of the drive wheels, depending on the moment of inertia of the wheels and the engine; $\dot{\gamma}_i / i = 1 \div 4/$ - wheel angular velocity; $[\ddot{\gamma}]$ - a matrix-column of the actual angular acceleration of the wheels, two or four of which are propulsive; M_{di}, M_{si} - corresponding engine and brake torque applied to each wheel.
Figure 10 shows the dynamic model of an active suspension system. Figure 11 shows the dynamic diagram of a driving or sliding wheel.
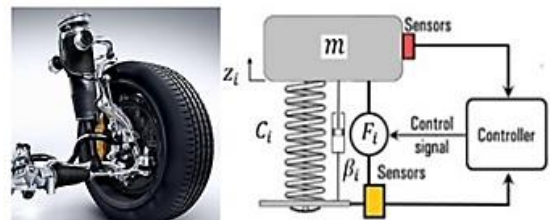

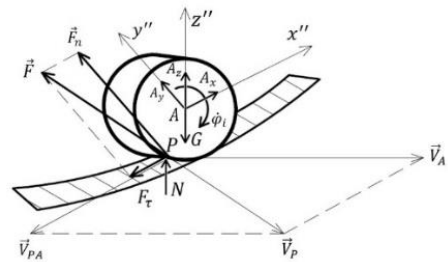**Figure 10.** Dynamic model of an active suspension system

Figure 11. Drive wheel diagram

The solutions of the system of differential equations of motion (8) are shown graphically (Fig.12-15).
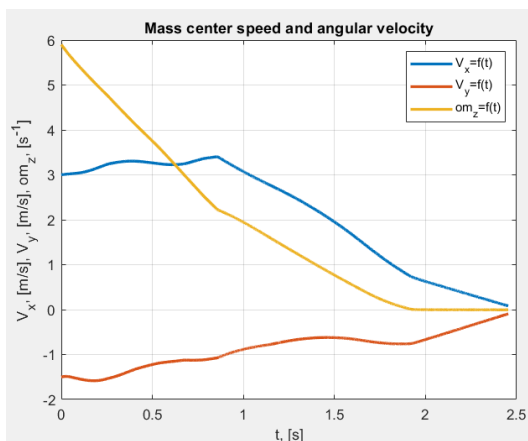
Figure 12. Change in the projections of the velocity of the center of mass and the angular velocity about a vertical axis after impact
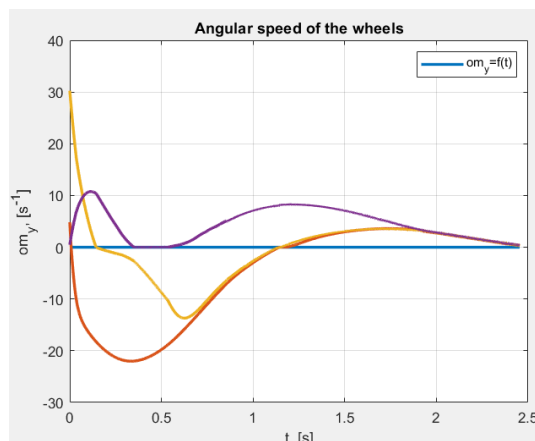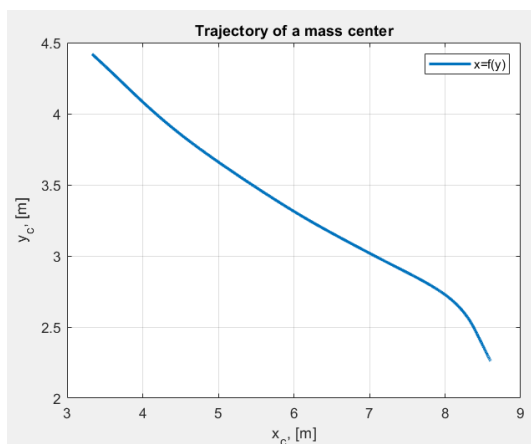

Figure 13. Trajectory of the vehicle center of mass after the impact
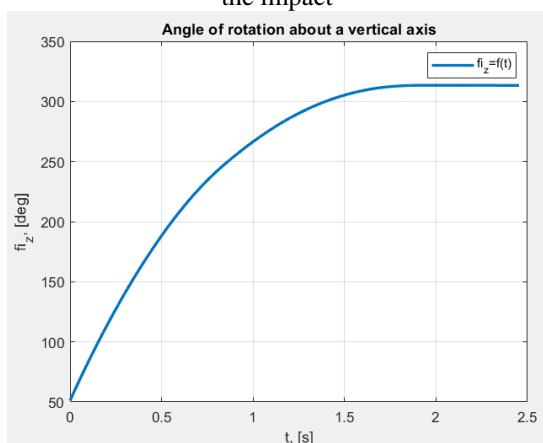
Figure 14. Post-impact change in the angle of rotation about a vertical axis

Figure 15. Post-impact change in the wheels angular velocity

During impact, the fictitious translation forces are dominant for each of the bodies. This is due to the incredibly higher translation acceleration during impact. After the impact and the subsequent motion of the cars, inertial forces are commensurate with each other in size, changing their direction in relation to the vehicle body (Fig. 16).
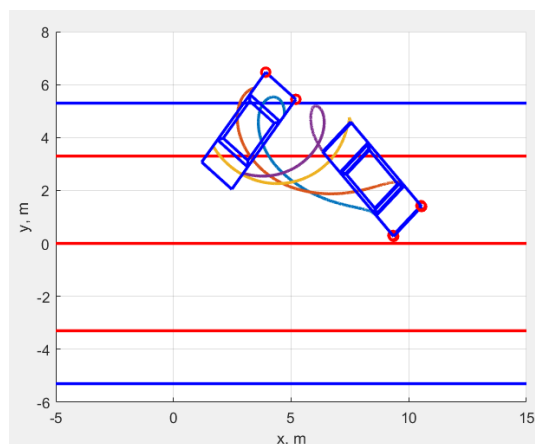

Figure 16. Discrete positions of vehicle's motion

The first emerging main component of the fictitious translation force is the impact force, which is due to the acceleration of the center of mass at the stage of impact deformation. The car motion is mainly translational, without sensitive rotation (Fig. 17). The fictitious translation force has the form

$$\vec{F}_{ec} = -m.\vec{a}_{cy1} = -\frac{m}{\tau}.d\vec{V}, \qquad (13)$$

where τ is the time of impact; $\vec{a}_{cy1}$ - acceleration of the center of mass during impact; $d\vec{V}$ - change of the speed of the car center of mass. This force component arises first at impact and decreases sharply after it when the maximum deformation is reached.
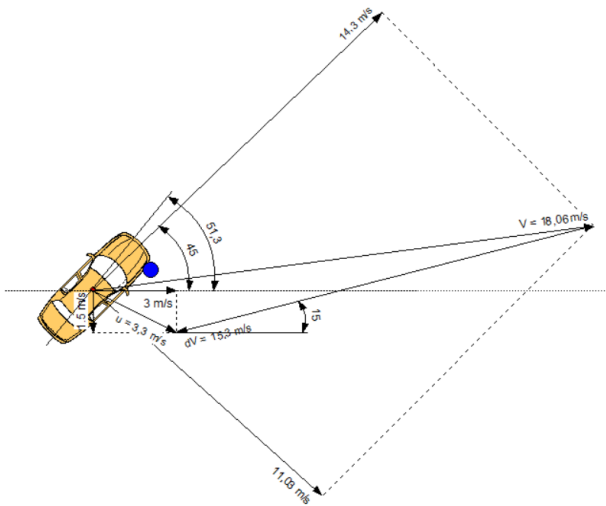
Figure 17. Vector plan of change of the velocity of the center of mass at impact

$$m.\vec{u} - m.\vec{V} = \vec{S}. \tag{14}$$

Here $\vec{u}$ is the velocity of the vehicle center of mass after the impact; $\vec{V}$ - the vehicle velocity of the center of mass immediately before the impact; $\vec{S}$ – vehicle crash pulse. According to the theorem, the vehicle velocity of the center of mass varies in position, magnitude and direction, and its change is determined by the expression

$$\vec{u} - \vec{V} = \overrightarrow{\Delta V}. \tag{15}$$

The magnitude of this force for the driver and the bodies of the passengers is indicative:

$$|\vec{F}_{ec}| = \left| -\frac{m_p}{\tau}.dV \right| = \frac{80}{0,025}.15,3 = 48960N. \tag{16}$$

Under the action of this very great force, the bodies tend to move forward and slightly to the right at an angle of about 15 to the vehicle longitudinal axis. The movement itself depends on whether the passenger in question is wearing a seat belt. The reported direction of motion of the bodies is in the direction of the velocity of the center of mass.

The other main component of the fictitious translation force acting on the bodies in the car is the fictitious translation force due to the rotational component of the motion, respectively the post-impact vehicle angular velocity/ centrifugal inertial force/. Its size is determined by the formula

$$F_{e\omega} = m_p.\rho.\omega_z^2, \tag{17}$$

where ρ is the distance from the body center of mass to the vehicle center of mass at the moment of impact/this distance consequently changes with the movement of the bodies in the car/. Its size at the initial moment of rotation is as follows:

$$F_{e\omega} = 80.1.5,9^2 = 2785 \ N. \tag{18}$$

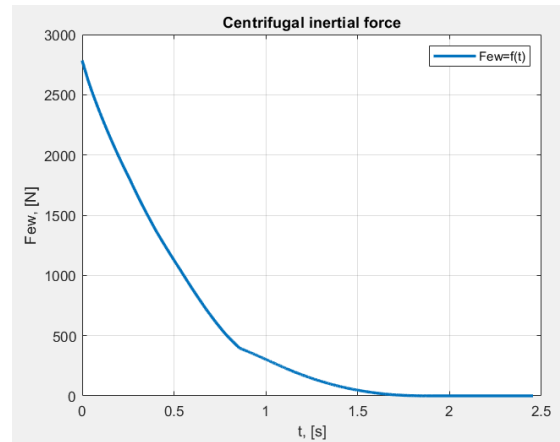The change in centrifugal inertial force has the form shown by graphical dependence (Fig. 18).

Figure 18. Graphic dependence of the centrifugal inertial force

Coriolis inertial forces are also important during the car rotation as well as the body displacement inside the cabin. The relative velocity of the body displacement inside the compartment can be determined according to the work-energy theorem when the resistance is neglected. It has the form of:

$$\frac{m_p.V_r^2}{2} = \int_{x_o}^{x_1} m_p.\omega_z^2.x.dx \ ; \tag{19}$$

$$V_r = \sqrt{x_1^2 - x_o^2}.\omega,$$

where x_1 and x_o are the respective distances from the body center of mass to the vehicle center of gravity at the time of impact and for a given moment while the vehicle is moving.

The Coriolis force has the magnitude of

$$F_c = 2.m_p.\omega.V_r = 2.m_p.\sqrt{x_1^2 - x_o^2}.\omega^2. \tag{20}$$

The Coriolis force with passenger displacement at 0,2 m has the approximate magnitude of

$$F_c = 2.m_p.\omega.V_r =$$
$$= 2.80.\sqrt{1^2 - 0,8^2}.5,9^2 = 3342 \ N. \tag{21}$$

Total forces generated by the angular velocity (centrifugal forces) and the Coriolis acceleration (Coriolis forces) have the form of

$$\vec{F}_{e\omega c} = \vec{F}_{e\omega} + \vec{F}_c. \tag{22}$$

The dynamic analysis shows that the passenger in the car has moved strongly forward and slightly to the right in the compartment, massively deforming the front right door. The motion of the passenger's body is determined initially by the incredibly higher fictitious translation force at impact stage, and then in the motion with rotation around a vertical axis the centrifugal inertial force is of primary importance (Fig. 19 - 20).
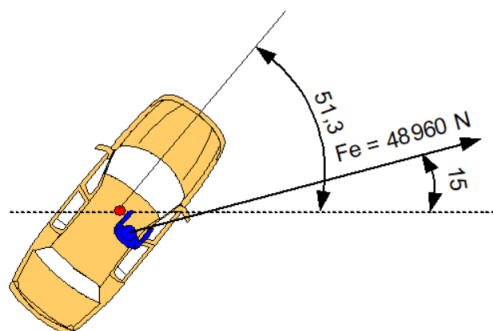

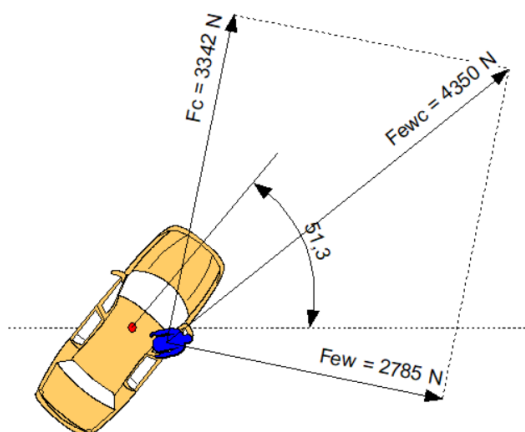**Figure 19.** Direction of action of the fictitious translation force at impact stage

Figure 20. Post-impact direction of action of the centrifugal and Coriolis inertial forces

According to the performed dynamic study, it is clear that there are two main directions of motion of the front passenger in the right seat. The first is when moving forward and to the right in the passenger compartment, and the second is when going out of the passenger compartment through the front right door glass as a result of the action of the total vector of centrifugal inertial force and Coriolis inertial force. If the passenger in the car had been wearing a seat belt, he would not have gone out of the car body, but would have maintained a relatively balanced position on the front right seat.

3. CONCLUSION

1. Dynamic analysis of the impact phase of a vehicle-fixed barrier collision has been performed by the finite element method using the software product Abaqus/Explicit.

2. Solution to Cauchy problem on the study of the impact process dynamics when hitting a fixed barrier has been found, as the initial kinematic values at the time of impact meet the final positions at rest in the post-impact vehicle macromotion.

3. Dynamic analysis of the action of the main inertial forces during and after impact has been performed.

4. The effect of inertial forces on the bodies of passengers at the impact phase of a vehicle-fixed barrier collision has been determined.

5. The influence of seat belts use on the action of inertial forces when hitting a fixed barrier has been determined.

References:

Daily, J., Shigemura, N. S., & Daily, J. (2006). *Fundamentals of traffic crash reconstruction.* Jacksonville, Florida: Institute of Police Technololgy and Managment, University of North Florida

Dechkova, S. (2018). Creation of multi-mass models in the SolidWorks and Matlab environment for crash identification. *Machine Mechanics*, *119*, 28-32.

Jiang, T., Grzebieta, R. H., Rechnitzer, G., Richardson, S., & Zhao, X. L. (2003). Review of car frontal stiffness equations for estimating vehicle impact velocities. In *Proceedings: International Technical Conference on the Enhanced Safety of Vehicles* (Vol. 2003, pp. 11-p). National Highway Traffic Safety Administration.

Karapetkov, S., & Dimitrov, L. (2022). An Update on the Momentum 360 Method of Vehicle Impact Reconstruction through 3D Modeling and Computer Simulation. *Symmetry*, *14*(12), 2628. https://doi.org/10.3390/sym14122628

Karapetkov, S. (2010). *Investigation of road traffic accident, technical commentary on the lawyer*. Technical University of Sofia, Bulgaria.

Karapetkov, S., & Uzunov, H. (2016). *Dynamics of transverse resistance of a car*. Didada Consult–Sofia, Bulgaria.

Karapetkov, S., Dimitrov, L., Uzunov, H., & Dechkova, S. (2019). Identifying vehicle and collision impact by applying the principle of conservation of mechanical energy. *Transport and Telecommunication Journal*, *20*(3), 191-204.

Karapetkov, S., Dimitrov, L., Uzunov, H., & Dechkova, S. (2019). Examination of vehicle impact against stationary roadside objects. 9*th International Scientific Conference on Research and Development of Mechanical Elements and Systems, IRMES* 2019, University of Kragujevac, Faculty of EngineeringKragujevac; Serbia; 5 September 2019 through 7 September 2019; Code 154497, Kragujevac, Serbia

Kolev, Z. D., & Kadirova, S. Y. (2019, September). Numerical modelling of heat transfer in convector's pipes by ABAQUS. In *IOP Conference Series: Materials Science and Engineering* (Vol. 595, No. 1, p. 012006). IOP Publishing. https://www.scimagojr.com/journalsearch.php?q=19700200831&tip=sid), ISSN1757-899X (Online)

Kolev, Z., & Kadirova, S. (2020). Numerical modeling of the thermal conduction process in water-air convector's fins. In *E3S Web of Conferences* (Vol. 180, p. 01009). EDP Sciences. https://doi.org/10.1051/e3sconf/202018001009), E-ISSN 2267-1242

Lyubenov, D., Mateev, V., & Kadikyanov, G. (2019). An expert system for vehicle accident reconstruction. *IOP Conference Series: Materials Science and Engineering, 2019, 614*(1), 012006. DOI 10.1088/1757-899X/614/1/012006. ISSN 17578981

Lyubenov, D., Balbuzanov, T., & Dinolov, O. (2022, August). Application of GPS-based information system in studying dynamic properties of vehicles. In *AIP Conference Proceedings, 2570*(1). AIP Publishing. doi 10.1063/5.0100026. ISBN978-073544375-4

Matzinski, P., Uzunov, H., Dimitrov, K., & Dechkova, S. (2021). Training methodology for forensic engineering experts in traffic accident investigation - problem-oriented approach. Uni*on of scientists in Bulgaria - branch Sliven, 36*. pp. 58-64, Kavarna. ISSN 1311-2864.

Niehoff, P., & Gabler, C. (2006). The Accuracy of WinSMASH Delta-V Estimates: The Influence of Vehicle Type, Stiffness, and Impact Mode." In *the 50th Annual Proceedings of the Association for the Advancement of Automotive Medicine, 50*, 73-89, Chicago, IL

Owsiański, R. (2007). Szacowanie energii deformacji nadwozi kompaktowych samochodów osobowych (Estimation of the bodywork deformation energy of compact passenger cars). *Paragraf na Drodze*, *4*.

Saliev, D. N., & Damyanov, I. S. (2022, September). Vehicles acceleration rate study for intergreen time of a signal cycle compute. In *AIP Conference Proceedings*, *2449*(1). AIP Publishing. https://doi.org/10.1063/5.0091882

Schmidt, B., Haight, W., Szabo, T., & Welcher, J. (1998). System-based energy and momentum analysis of collisions. In *Accident Reconstruction: Technology and Animation* VIII SP-1319, no. 980026, Society of Automotive Engineers, Warrendale, PA, February

Sharma, D., Stern, S., Brophy, J., & Choi, E. (2007, June). An overview of NHTSA's crash reconstruction software WinSMASH. In *Proceedings of the 20th International Technical Conference on Enhanced Safety of Vehicles*. Paper No. 07-0211, Lyon, France

Stronge, W. (2000). *Impact Mechanics*. Cambridge: Cambridge University Press

Uzunov, H., Dechkova, S., Dimitrov, K., & Uzunov, V. (2021). Mechanical Mathematical Modelling of a Car Accident Caused by Sudden Mechanical Failure. *Journal of Engineering Science & Technology Review*, *14*(4), 61 – 68. doi: 10.25103/jestr.144.08

Uzunov, Hr., Dimitrov, K., & Dechkova, S. (2022). Experimental Determination of the Tire-Road Friction Coefficient for a Vehicle with Anti-Lock Braking System. 13th International Scientific Conference on Aeronautics, Automotive and Railway Engineering and Technologies (BulTrans-2021). *AIP Conf. Proc. 2557*, 030001-1–030001-11. https://doi.org/10.1063/5.0103769

Uzunov, H., Matzinski, P., Dechkova, S., & Dimov, N. (2021). Systems engineering information model of vehicle-pedestrian collisions. *Cybernetics and information technologies*, *21*(1), 151-168.

Wach, W. (2003). Analiza deformacji samochodu według standardu CRASH3. Część 2: Pomiar głębokości odkształcenia (Analysis of motor vehicle deformation according to the CRASH3 standard. Part 2: Measurement of deformation depth). Paragraf na Drodze No. 12

Stanimir Karapetkov
Technical University of Sofia, Faculty
and College – Sliven,
Sliven,
Bulgaria
skarapetkov@yahoo.com

Hristo Uzunov
Technical University of Sofia, Faculty
and College – Sliven,
Sliven,
Bulgaria
hvuzunov@gmail.com
ORCID 0000-0003-2229-2828

Silvia Dechkova
Technical University of Sofia, Faculty
and College – Sliven,
Sliven,
Bulgaria
silviadechkova@gmail.com
ORCID 0000-0002-1784-6956

Vasil Uzunov
Technical University of Sofia, Faculty
and College – Sliven,
Sliven,
Bulgaria
xavi66@mail.bg